Northern Hemisphere atmospheric blocking in ice core accumulation records from Northern Greenland

Norel Rimbu[1], Gerrit Lohmann[1,2], Klaus Grosfeld[1]

[1] Alfred Wegener Institute for Polar and Marine Research, 27570 Bremerhaven, Germany.

[2]DFG Research Center for Ocean Margins, University of Bremen, 28359 Bremen, Germany.

Short title:

Abstract.

We investigate the connection between frequency of atmospheric blocking circulation and the variability of five high resolution accumulation records from Northern Greenland. It is shown that during years of high ice accumulation records the frequency of winter blocking circulation in the Euro-Atlantic region is significantly higher relative to the years of low accumulation. Our results show an enhanced Greenland storm track as well as enhanced moisture transport toward Greenland during the periods of high blocking activity relative to the periods of low blocking activity. The time series associated with the dominant mode of accumulation variability shows significant multidecadal variations during the last five centuries. We suggest that positive (negative) phase of these multidecadal oscillations are related to high (low) blocking activity in the Euro-Atlantic region.

1. Introduction

During the last decade interest in the variability of high-resolution ice core data has increased markedly as its connection to regional and global atmospheric circulation variability has become more and more evident (Rogers et al., 2004; Hanna et al., 2006). In particular, it has been shown that local ice core accumulation variability is largely controlled by atmospheric circulation variability (Crüger et al., 2004).

Many studies reveal a direct connection between large-scale atmospheric circulation anomaly patterns and interannual accumulation variability in Greenland. The North Atlantic Oscillation (NAO), the dominant pattern of North Atlantic climate variability, is significantly negatively correlated with accumulation records from west-central Greenland during the period 1856-1992 (Appenzeller et al., 1998). Analysis of snow accumulation rates data from the European Center for Medium Range Forecast (ERA40) reveals that positive accumulation anomalies from the northeastern and southwestern Greenland Ice Sheet are connected to a high-pressure bridge that extends from the central North Atlantic to Scandinavia. Positive accumulation anomalies in southeastern Greenland are associated with a blocking-like pattern with a center over Northern Scandinavia to Spitsbergen (Hutterli et al., 2005).

Besides regional and large-scale atmospheric circulation patterns, accumulation variability in Greenland is related to the variability of cyclone frequency. Rogers et al. (2004) show that cyclone frequency variations are significantly related to the primary modes of Greenland snow accumulation. A significant impact of the variability of frequency and strength of cyclones originating from the Greenland Sea in the snow accumulation on north-eastern Greenland Ice Sheet was also detected (Hutterli et al., 2005).

Atmospheric blocking is inherent to Northern Hemisphere atmospheric circulation variability. It is defined as a long-lived and recurrent system embedded within the latitude belt of baroclinic westerlies (e.g., Tibaldi et al., 1997). The frequent occurrence and prolonged duration of blocking exert a strong impact on regional and global circulation systems. It is the goal of this study to investigate how the variability of Northern Hemisphere blocking is related to ice core accumulation variability of several high-resolution accumulation records from northern Greenland (Schwager, 2000). A direct connection between Northern Hemisphere blocking activity and long-term high-resolution ice core records could give valuable information on the variability of the frequency of this atmospheric circulation regime during the pre-instrumental period.

Data and methods

The Alfred Wegener Institute for Polar and Marine Research (AWI) in Bremerhaven (Germany) performed a North Greenland Traverse (NGT) between 1993 and 1995 (Schwager, 2000). In this paper we refer to the yearly snow accumulation time series of five ice cores drilled during the NGT. These records are located in northern Greenland (Fig. 1a) and referred to as : B16 (73.9°N, 37.6°W), B18 (76.6°N, 36.4°W), B21 (80.4°N, 41.1°W), B26 (77.3°N, 49.2°W) and B29 (76.0°N, 43.5°W) and reach depths of up to 150 m. Mean accumulation rates varies between 104±32 $mm_{w.e.}$ a^{-1} and 179±49

$mm_{w.e.}$ a^{-1}. These records cover various periods of the last millennium (Schwager, 2000). The longest period is covered by B18 (871-1992) and the shortest by B26 (1502-1994). We analyze the accumulation variability in these ice cores during their common period, which is 1502-1992. These accumulation time series are available through the PANGAEA online environmental data base (http://www.pangaea.de). The dominant pattern of the variability in these ice cores is based on Empirical Orthogonal Function (EOF) analysis (von Storch and Zwiers, 1999). The EOFs are constructed using normalized accumulation time series for the period 1502-1992. The associated coefficient time series (PC1) was normalized by its standard deviation.

The climatic data used in this study were obtained from the 2.5° x 2.5° NCEP/NCAR reanalysis (Kalnay et al., 1996) for 1948-1992. We used the daily mean 500 hPa heights (Z500) to compute the blocking frequency during the 44 winter (DJF) seasons. Using the daily mean Z500 we calculate the Tibaldi-Molteni index (TM; Tibaldi and Molteni, 1990) as follows. For each longitude the southern Z500 gradients (GHGS) and the northern Z500 gradients (GHGN) are computed as follows:

$$GHGS = (Z(\Phi_0) - Z(\Phi_s))/(\Phi_0 - \Phi_s)$$

$$GHGN = (Z(\Phi_n) - Z(\Phi_0))/(\Phi_n - \Phi_0)$$

where $\Phi_n = 80°N + \Delta$, $\Phi_0 = 60°N + \Delta$, $\Phi_s = 40°N + \Delta$, Δ = -5°, 0°, 5° latitude. A given longitude is blocked if the following conditions are satisfied for at least one value of Δ:

$$GHGS > 0 \text{ and } GHGN < -10 \text{ m/° latitude.}$$

Further, the ratio of the blocked days at a certain longitude to the number of winter season days (DJF, 90 days) is referred to as the local blocking frequency (LBF).

To assess the statistical significance of the LBF obtained for high (PC1 higher than 0.5 standard deviation) and low (PC1 lower than -0.5 standard deviation) accumulation years, we tested the validity of the null hypothesis that the difference between LBF corresponding to high and low accumulation years is indistinguishable from zero. We generate 1000 synthetic time series constructed to have the same variance and autocorrelation function as the accumulation PC1 for the period 1948-1992 using a first-order autoregressive model (AR1). Based on the 1000 LBF distributions corresponding to these synthetic time series we established the 90% significance level (Fig. 2b; dashed curves). The significance of the LBF differences was confirmed by an independent analysis based on a t-test (von Storch and Zwiers, 1999).

Because blocking circulation is characterized by time persistency as well as spatial extension over several longitudes, additional criteria should be considered to identify blocking events (Barriopedro et al., 2006). Here we consider a sector to be blocked if three or more consecutive longitudes are blocked according to the TM index for at least five consecutive days. In our study, high (low) blocking activity in a certain sector is associated with values of the blocking index higher (lower) than +1.0 (-1.0) standard deviation.

In our study we also use the field of Z500 standard deviation derived from the daily Z500 winter field band pass filtered in the 2.5-6 day (STD500) to identify the storm track. The filter restricts the variability to the characteristic time scale of synoptic cyclones, but a considerable amount of anomalies which are not related to cyclones, e.g., waves and high-pressure systems, is included (Luksch et al., 2005). Another climatic field used in our study is the vertically integrated water vapors transport (WVT; Peixoto and Oort, 1992) for the period 1948-1992. For each vertical layer and each grid-point of NCEP/NCAR model the WVT was calculated as the product between the mean values of horizontal wind and specific humidity corresponding to lower and upper pressure level respectively weighted with the layer's thickness divided by the gravity. The vertically integrated WVT was obtained by summation of WVT for all layers located between the Earth's surface and 300 mb surface. Above 300 mb the specific humidity in the the NCEP/NCAR model is zero (Kalnay et al., 1996). The maps of mean STD500 and vertically integrated WVT corresponding to the winters characterized by high and low blocking activity are constructed and analyzed in order to identify the physical mechanisms behind the connection of accumulation to atmospheric blocking variability. We use winter climatic fields because atmospheric circulation and ice accumulation are found to be most significantly related during this season (Rogers et al., 2004).

Results

The first EOF of the five accumulation records considered in our study (Fig. 1a), which explains 23% of the variance, captures in-phase variability of all accumulation records. Note that the EOF analysis was performed using normalized accumulation time series from the entire 1502-1992 period (491 years). Its associated time coefficients (PC1) show important interannual and decadal variations during the period 1502-1992

(Fig. 1b). The higher order EOF's (not shown) have a heterogeneous spatial structure and are not analyzed in this study.

The composite distributions of the LBF for high-accumulation years as well as for low-accumulation years during the period 1948-1992 are shown in Fig. 2a. The LBF during both, high and low accumulation years, is relatively high in the Euro-Atlantic and Pacific regions, respectively. Similar results are obtained when more complex blocking indices are used (e.g., Barriopedro et al., 2006). However, during high-accumulation years the LBF is significantly (90% level) higher than during low-accumulation years (Fig. 2b) for most of the longitudinal grid-points in the Euro-Atlantic region (20°W-80°E). From 80°W to 20°W the LBF is higher for low relative to high-accumulation years. No significant (90% level) differences between LBF during high and low accumulation years are detected in the Pacific sector (Fig. 2b). This suggests that positive anomalies of the accumulation records considered in our study are related to enhanced blocking activity in the Euro-Atlantic region. Low blocking activity in this sector is associated with negative accumulation anomalies.

Because the difference in LBF distributions between high and low accumulation years is the highest around 0° longitude, we define a blocking index as the normalized frequency of blocked days when the longitudes 0°, 2.5°E and 5°E are consecutively blocked for at least five days. The resulting time series (Fig. 3a) shows important interannual and decadal variability. Similar variations of blocking activity in this region were identified by Tibaldi et al. (1997). The blocking index and the corresponding composite maps are calculated using NCEP/NCAR data (Kalnay et al., 1996) from

1948 to 2005 (57 winters) in order to improve the statistical significance of the patterns.

To identify the physical mechanism responsible for the connection between accumulation and blocking variability, we construct the mean maps of STD500 field for the years of high and respectively low values of the blocking index represented in Fig. 3a. The difference between the high and low STD500 composite maps shows positive anomalies over a large area of the northern part of the North Atlantic region, including Greenland (Fig. 3b). The enhanced synoptic scale activity in this region during high blocking activity is consistent with high snow accumulation in northern and north-eastern Greenland, where our accumulation ice core records are located.

To better assess the relation between blocking activity and our accumulation records, we investigate the moisture transport in the North Atlantic region during high and low accumulation years. Vector plots of the vertically integrated total WVT composites (Fig. 4a) show that during times of high blocking frequency the axis of maximum moisture transport shifts to a more northeast directed orientation across the Atlantic and extends northward to Greenland relative to the times of low blocking frequency (Fig. 4b). A significant reduction of the magnitude (contour lines) of atmospheric moisture transport over Greenland during low relative to high blocking activity in this region is also evident (Fig. 4).

Discussion

In this study we investigate the relation between the dominant mode of accumulation variability from five high resolution northern Greenland ice cores and the blocking activity in the Northern Hemisphere. Recent studies (Krabill et al., 2004; Hanna et al., 2006) show that unusually high accumulation in southeast Greenland in 2002/2003 winter was related to a persistent blocking anticyclone centered over Scandinavia. Weather systems were dragged up over southeast Greenland dumping a lot of snow in the region during this particular winter. This case study is consistent with enhanced synoptic activity over Greenland during high blocking activity in the Euro-Atlantic region as described in our study. Furthermore, our blocking index (Fig. 3a) shows relatively high value during 2002/2003 winter. It shows also relatively high values in the 1971/1972 and 1963/1964 winters when high accumulation were recorded in southeast Greenland (Hanna et a., 2006). Morever, the high accumulations recorded in 1996 in both northwest and southeast Greenland (Rogers et al., 2004) may be related to enhanced blocking activity during the winter 1995/1996 as indicated by our blocking index (Fig. 3a). As Fig. 3b shows, high blocking activity in the Euro-Atlantic region is related to enhanced STD500 over much part of Greenland, consistent with the monopolar structure of the dominant pattern of the variability of our accumulation records (Fig. 1a). However, relatively short accumulation records from different parts of Greenland Ice Sheet tend to be weak correlated each other (Crüger et al., 2004; Hutterli et al., 2005). We suggest that long enough accumulation time series, like the ones considered in our study, should be used in the statistical analysis in order to separate the large-scale climatic signal from local meteorological and glaciological noise.

Several studies (Appenzeller et al., 1998; Rogers et al., 2004) show that the NAO is significantly correlated with accumulation anomalies from several parts of Greenland

Ice Sheet. The accumulation PC1 (Fig. 1b) is not significantly correlated (r=+0.1) with the winter NAO index (Hurrell et al., 2003) for the period 1864-1992. Negative NAO phase is associated to relatively high blocking activity from 90°W to 10°E as well as with a slightly increase in blocking activity from 10°E to 80°E. The blocking anomaly pattern for high accumulation years (Fig. 2b) shows low blocking activity from 80°W-20°W as well as enhanced blocking activity from 20°W-80°E which strongly resembles the blocking anomaly distribution associated to the positive phase of the Scandinavian pattern (Barriopedro et al., 2006; their Fig. 9)). Therefore the relatively low correlation between accumulation PC1 and NAO may be related to relatively weak projection of the blocking pattern associated to NAO and to our accumulation records.

Distinct synoptic scale processes control accumulation variability in different regions of the Greenland Ice Sheet. Lee cyclogenesis is important in precipitation production over southern and eastern Greenland (Rogers et al., 2004), while cyclones originating in the Greenland Sea control the accumulation variability in north-eastern Greenland (Hutterli et al., 2005). We argue that an enhanced blocking activity in the Euro-Atlantic region is related to an enhanced advection of warm and moist air toward Greenland which leads to increase in precipitation via increase in the cyclogenesis. This is in agreement with the simulation of the high resolution model HIRHAM4 (Dethloff et al., 2002) showing more precipitation over Greenland in years with stronger cyclonic activity and less precipitation in years with reduced number of cyclones.

Analysis of observational data reveals significant trends as well as interannual and interdecadal variations of atmospheric blocking activity in different sectors of the Northern Hemisphere (e.g., Barriopedro et al., 2006). However, the long-term temporal patterns of blocking variability were established using data from the relatively short NCEP/NCAR period. Using our proxy data we try to put these variations into a long-term context. Prominent negative (positive) values of low pass filtered time coefficients associated with the dominant pattern of accumulation variability during the 1620s, 1700s and 1770s (1660s and 1740s) may be an indication of low (high) blocking activity in the Euro-Atlantic region during these periods (Fig. 1b). Significant anomalies in blocking activity during the pre-instrumental period were detected in reconstructed data as well in model experiments (Casty et al., 2005). Fig. 1b shows enhanced accumulation variability at multidecadal time scales of 70-90 years, which is also confirmed by spectral analysis (not shown). Based on the connection between blocking activity and accumulation variability established in our study, we suggest that Euro-Atlantic blocking activity during winter is also characterized by multidecadal variations with a 70-90 year characteristic time scale. These variations can be related to coupled atmosphere-ocean-ice interactions in the North Atlantic, which generate variability at these time scales (Dima et al., 2007) or probably related to a solar influence on North Atlantic multidecadal variability (Lohmann et al., 2004).

High-resolution and long-term ice core data as analyzed here offer estimations of the variability of the atmospheric blocking circulation regime during the past five centuries. However, combined studies of reconstructions and model simulations are necessary to improve our understanding of past variability of the atmospheric circulation blocking regime.

Acknowledgments: This study was funded by grants from the German Ministry of Research and Education (BMBF) through the program MARCOPOLI (MAR2). We are grateful to M. Schwager for providing the high resolution ice core data. We thank the reviewers for their constructive comments.

References

Appenzeller, C., T.F. Stocker, and M. Anklin (1998), North Atlantic Oscillation dynamics recorded in Greenland ice cores, *Science, 282*, 446-449.

Barriopedro, D., R.G. Herrera, A.R. Lupo, and E. Hernández (2006), A climatology of Northern Hemisphere blocking, *J. Clim., 19*, 1042-1063.

Casty, C., D. Handorf, C.C. Raible, J.F. Gonzáles-Rauco, A. Weisheimer, E. Xoplaki, J. Luterbacher, K. Dethloff, and H. Wanner (2005), Recurrent climate winter regimes in reconstructed and modelled 500 hPa geopotential height fields over the North Atlantic/European sector 1659-1990, *Clim. Dyn., 24*, 809-822.

Crüger, T., H. Fischer, and H. von Storch (2004), What do accumulation records of single ice cores in Greenland represent?, *J. Geophys. Res., 109*, D21110, doi:10.1029/2004JD005014.

Dima, M., and G. Lohmann (2007), A hemispheric mechanism for the Atlantic Multidecadal Oscillation, *J. Climate, in press.*

Dethloff, K., M. Schwager, J.H. Christensen, S. Kilsholm, A. Rinke, W. Dorn, F. Jung-Rothenhäusler, H. Fisher, S. Kipfstuhl, and H. Miller (2002), Recent Greenland accumulation estimated from regional climate model simulations and ice core analysis, *J. Climate, 15*, 2821-2832.

Hanna, E., J. McConnell, S. Das, J. Cappelen, and A. Stephens (2006), Observed and modeled Greenland ice sheet snow accumulation, 1958-2003, and links with regional climate forcing, *J. Climate, 19*, 344-358.

Hutterli, M.A., C.C. Raible, and T.F. Stocker (2005), Reconstructing climate variability from Greenland ice sheet accumulation: An ERA40 study, *Geophys. Res. Lett., 32*, L23712, doi:10.1029/ 2005GL024745.

Hurrell, J.W., Y. Kushnir, M. Visbeck, and G. Ottersen (2003),. The North Atlantic Oscillation: Climate Significance and Environmental Impact,*An Overview of the North Atlantic Oscillation, J.W. Hurrell, Y. Kushnir, G. Ottersen, and M. Visbeck, Eds. Geophysical Monograph Series, 134*, 1-35.

Kalnay, E., and 21 coauthors (1996), The NMC/NCAR 40-Year Reanalysis Project. *Bull. Amer. Meteor. Soc., 77*, 437-471.

Krabill, W., E. Hanna, P. Huybrechts, W. Abdalati, J. Cappelen, B. Csatho, E. Frederick, S. Manizade, C. Martin, J. Sonntag, R. Swift, R. Thomas, and J. Yungel (2004), Greenland Ice sheet: Increased costal thinning, *Geophys. Ress. Lett., 31*, L24402, doi:10.1029/2004GL021533.

Lohmann, G., N. Rimbu, and M. Dima (2004), Climate signature of solar irradiance variations: Analysis of long-term instrumental, historical, and proxy data, *Int. Jour. Climatol., 24*, 1045 - 1056.

Luksch, U., C. Raible, R. Blender, and K. Fraedrich (2005), Decadal cyclone variability in the North Atlantic, *Meteorologische Zeitschrift, 14*, 747-753.

Peixoto, J. P., and A. H. Oort (1992), Physics of Climate, *American Institute of Physics, Springer-Verlag, New York,* 520 pp. .

Rogers, J.C., D. Bathke, E. Mosley-Thompson, S.-H. Wang (2004), Atmospheric circulation and cyclone frequency variations linked to the primary modes of Greenland snow accumulation, *Geophys. Res. Lett., 31*, doi: 10.1029/2004GL021048.

Schwager, M. (2000), Ice core analysis on the spatial and temporal variability of temperature and precipitation during the late Holocene in North Greenland, *Reports on Polar Research, Alfred Wegener Institute for Polar and Marine Research, Bremerhaven, 362*, 136 pp.

Tibaldi, S., and F. Molteni (1990), On the operational predictability of blocking, *Tellus, Ser A, 42*, 343-365.

Tibaldi, S., F. D'Andrea, E. Tosi, and E. Roeckner (1997), Climatology of the northern hemisphere blocking in the ECHAM model, *Clim. Dyn., 13*, 649-666.

von Storch, H., and F.W. Zwiers (1999), Statistical Analysis in Climate Research, *Cambridge University Press*, 494 pp.

Received ____________________

Figure 1. a) First EOF and b) the corresponding coefficient time series (thin) and its low frequency (time scales longer than 50 years) component (thick). The names of the core sites are indicated on the EOF map. The values written in brackets represent the correlation coefficient between PC1 and the corresponding normalized ice accumulation time series.

Figure 2. a) Frequency of winter blocked longitudes (LBF) for the years of high (solid) and low (dashed) ice accumulation, respectively. b) The difference between LBF corresponding to high and low ice accumulation years respectively (solid) and 90% significance level (dashed).

Figure 3. a) The time series of a blocking index defined as the normalized number of days during a winter for which the 0°, 2.5°E and 5°E longitudes were consecutively blocked for at least 5 days. b) Difference between composite maps of standard deviation of daily Z500 field filtered in the 2.5-6 days band associated with high and low values of the blocking index. Fill circles indicate the core sites. Units are m.

Figure 4. Composite map of the vertically integrated water vapors transport (vectors) and its magnitude (contour lines) for a) high and b) low values of the blocking index. Fill circles indicate the core sites. Units are kg/(ms).

a)

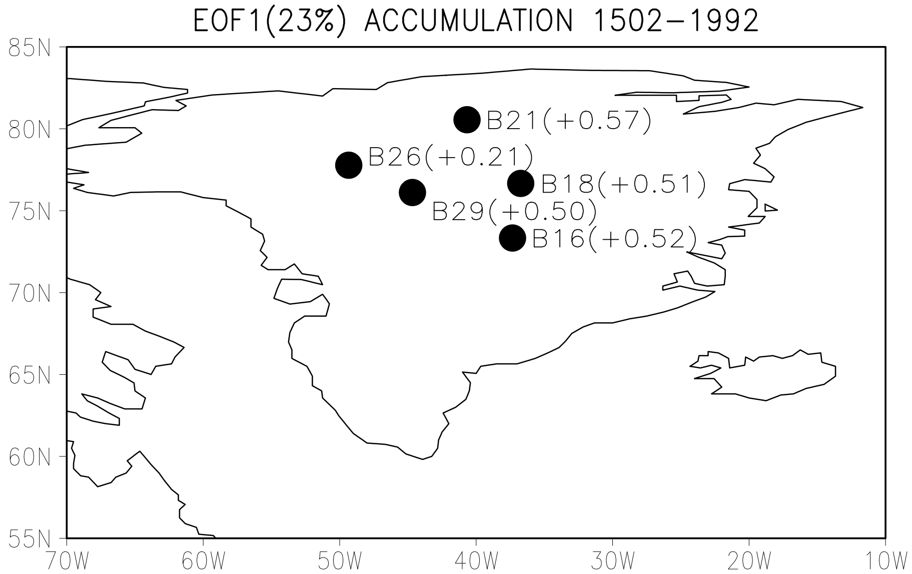
EOF1(23%) ACCUMULATION 1502-1992
85N
80N
75N
70N
65N
60N
55N
70W
60W
50W
40W
30W
20W
10W
B21(+0.57)
B26(+0.21)
B18(+0.51)
B29(+0.50)
B16(+0.52)

b)

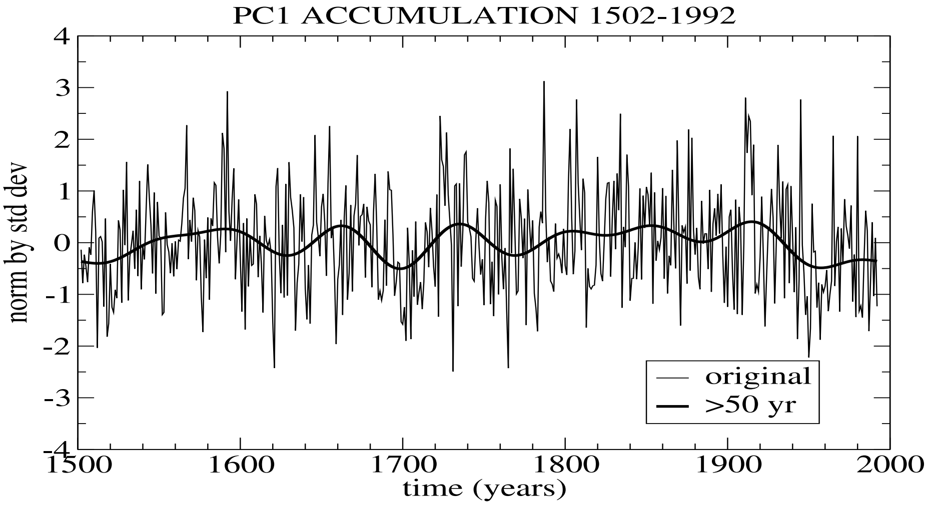
PC1 ACCUMULATION 1502-1992
norm by std dev
time (years)
original
>50 yr
4
3
2
1
0
-1
-2
-3
-4
1500
1600
1700
1800
1900
2000

a)

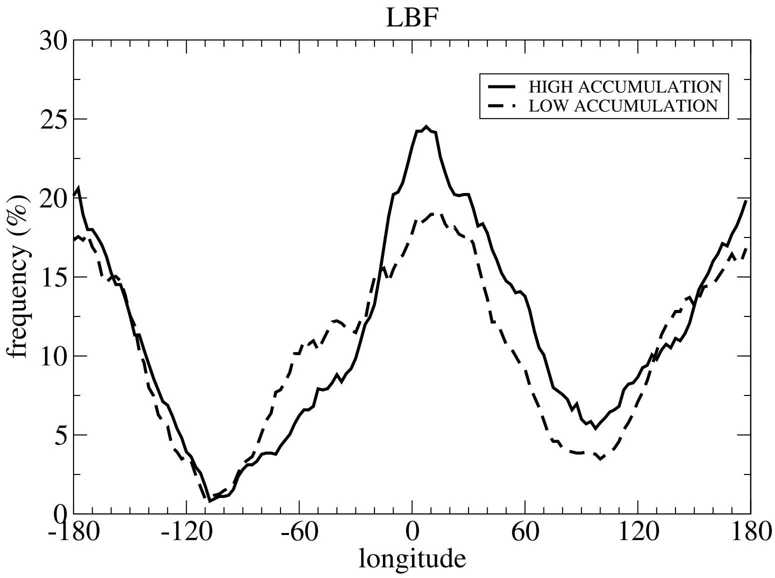
LBF
HIGH ACCUMULATION
LOW ACCUMULATION
frequency (%)
longitude
30
25
20
15
10
5
0
-180
-120
-60
0
60
120
180

b)

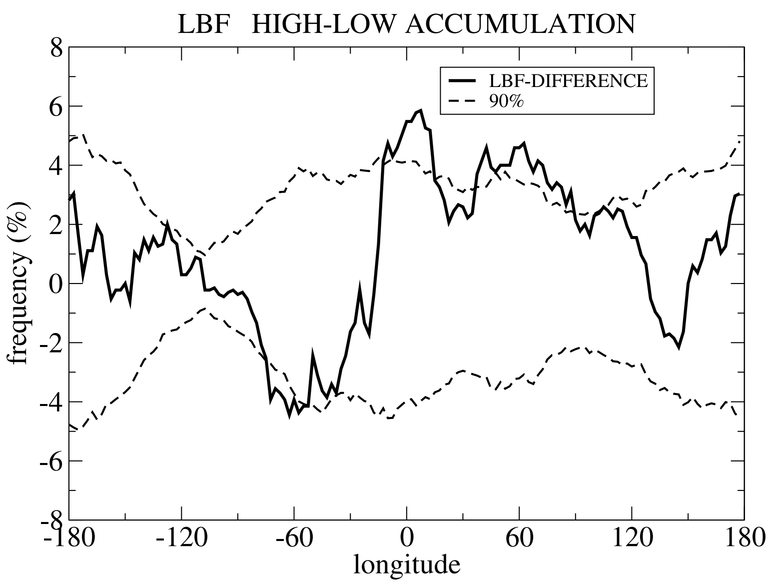
LBF HIGH-LOW ACCUMULATION
LBF-DIFFERENCE
90%
frequency (%)
longitude
8
6
4
2
0
-2
-4
-6
-8
-180
-120
-60
0
60
120
180

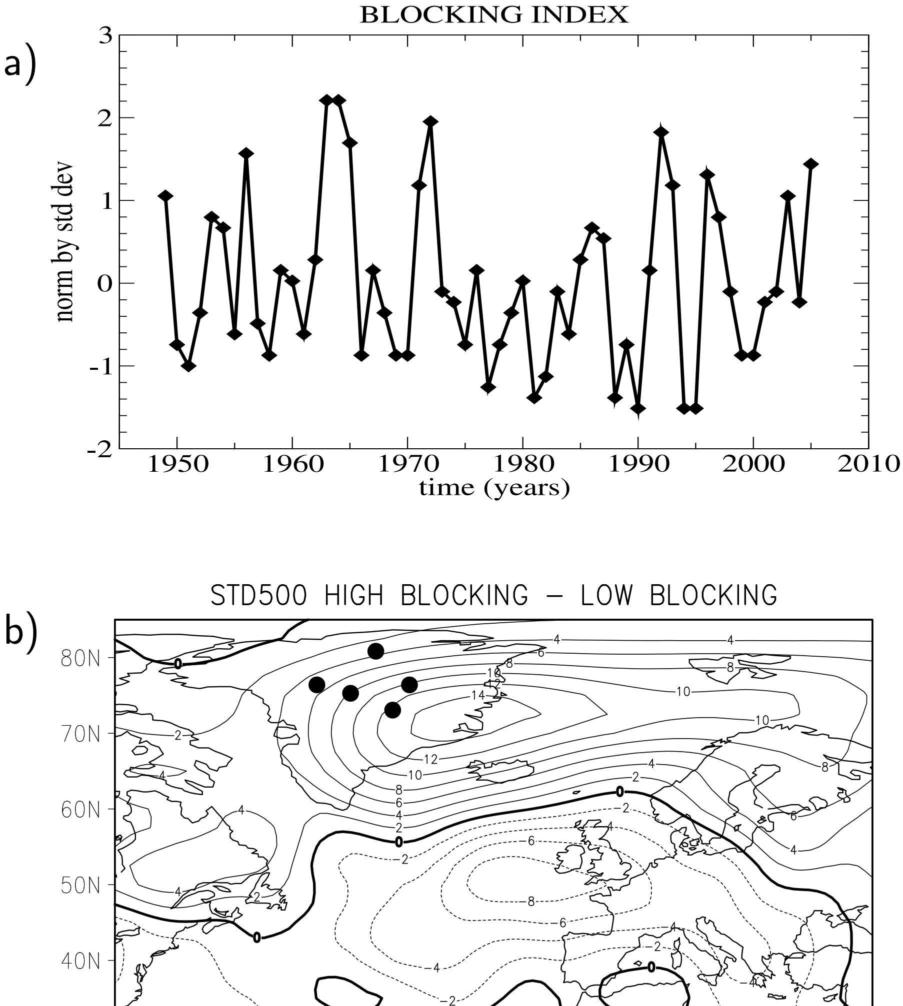
a)
BLOCKING INDEX
norm by std dev
time (years)
3
2
1
0
-1
-2
1950
1960
1970
1980
1990
2000
2010
b)
STD500 HIGH BLOCKING – LOW BLOCKING
80N
70N
60N
50N
40N
30N
80W
60W
40W
20W
0
20E
40E

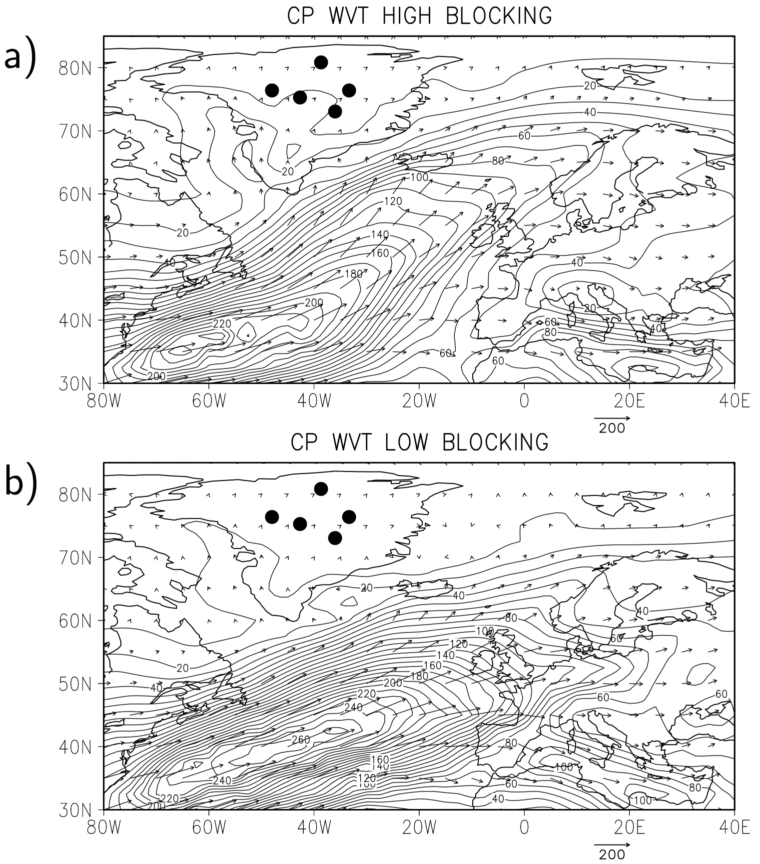
a)
CP WVT HIGH BLOCKING
b)
CP WVT LOW BLOCKING
80W
60W
40W
20W
0
20E
40E
30N
40N
50N
60N
70N
80N
200